

# Chirped pulse amplification in single mode Tm: fiber using a chirped Bragg grating

R. Andrew Sims · Pankaj Kadwani ·  
Heike Ebendorff-Heideprem · Lawrence Shah ·  
Tanya M. Monro · Martin Richardson

Received: 10 October 2012 / Accepted: 4 January 2013  
© Springer-Verlag Berlin Heidelberg 2013

**Abstract** We report femtosecond pulse generation and chirped pulse amplification in Tm: fiber. A mode-locked oscillator operating in the soliton regime produced 800 fs pulses with 5 nm spectral bandwidth, at 40 pJ pulse energy. This oscillator seeded a pre-amplifier that utilizes a Raman soliton self-frequency shift to produce wavelength tunable pulses with 3 nJ energy, reduced pulse duration of 150 fs, and increased bandwidth of 30 nm. For further amplification, the pulses were stretched up to 160 ps using a chirped Bragg grating (CBG). Stretched pulses were amplified to 85 nJ after compression in single-mode Tm: fiber and recompressed with the CBG as short as 400 fs. Compressed pulses were coupled into a highly nonlinear tellurite fiber to investigate the potential of this ultrashort pulse 2- $\mu$ m fiber source as a pump for mid-IR supercontinuum generation.

## 1 Introduction

Advancements in the development of femtosecond pulsed laser sources operating in the 2  $\mu$ m wavelength regime make them compelling pumps for mid-IR optical parametric oscillators [1] and supercontinuum generation [2]. The rate of development of Tm-doped ultrashort pulsed fiber sources has increased rapidly with mode-locking through numerous

techniques [3–6], pulse amplification via soliton self-frequency shift (SSFS) [1, 7, 8], and chirped pulse amplification (CPA) [9–12]. Using SSFS, sub-100 fs pulses operating at 75 MHz with 1 W of average power have been demonstrated and used to pump a broadband OPO [1]. Long stretching ratio CPA in thulium fiber has been demonstrated by two research groups to date; one reaching 151 nJ energy corresponding to  $\sim$ 600 kW peak power and the other generating 650 nJ pulses with  $\sim$ 800 kW peak power [10, 11]. In these cases, long lengths of passive fiber have been utilized to stretch pulse durations to 10's ps using both normal and anomalous dispersion fiber [10, 11] with grating-based compressors in Treacy or Martinez geometries, respectively. The next major performance threshold for Tm: fiber CPA systems is to exceed  $\mu$ J energy and/or MW peak power.

Here, we report a CPA system where pulses were generated and amplified in Tm: fiber, with pulse stretching and compressing using a chirped Bragg grating (CBG). The CBG offers the ability to use a single element for stretching and compressing of pulses via temporal reciprocity of the chirped structure in the Bragg grating. This CBG was fabricated in photo-thermo-refractive glass by Optigrate Corp. CBGs have been utilized previously at both 1 and 1.5  $\mu$ m, and achieving compressed pulses with 650 fs duration and 100 W average power at 1  $\mu$ m [13, 14]. To our knowledge, this is the first time a CBG has been used for CPA in the 2  $\mu$ m wavelength regime.

## 2 System design

### 2.1 Mode-locked oscillator

In this work, femtosecond pulses were generated in an all-fiber ring cavity pumped by an Er:Yb fiber laser. The

---

R. A. Sims (✉) · P. Kadwani · L. Shah · M. Richardson  
Townes Laser Institute, CREOL, The College of Optics  
and Photonics, University of Central Florida,  
4000 Central Florida Boulevard, Orlando, FL 32816, USA  
e-mail: rasims@creol.ucf.edu

H. Ebendorff-Heideprem · T. M. Monro  
Centre of Expertise in Photonics, Institute for Photonics  
and Advanced Sensing, University of Adelaide,  
Adelaide, SA 5005, Australia

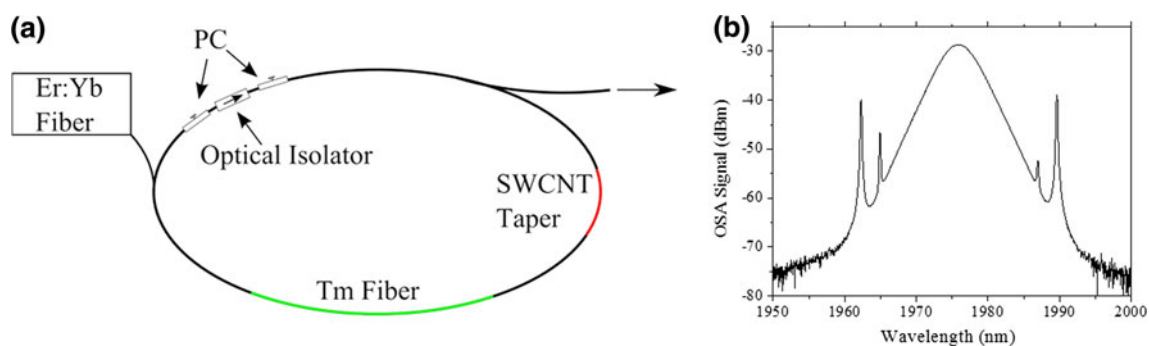


**Fig. 1** **a** All-fiber mode-locked Tm:fiber laser schematic. **b** Mode-locked oscillator spectrum

oscillator, shown in Fig. 1a, contains sections of SMF28E passive fiber and an uncooled section of  $\sim 1$  m long section of non-PM 10/130 Tm-doped fiber (Nufern). The oscillator was passively mode-locked using a single-walled carbon nanotube saturable absorber fiber taper [15] (KPhotonics, LLC) and polarization controllers in the system. Time-bandwidth limited pulses were output from the 90/10 tap coupler with pulse durations of  $\sim 800$  fs and 5 nm (FWHM) spectral bandwidth centered at 1,975 nm. Due to the anomalous dispersion of the fibers in the cavity, the oscillator operated in the soliton regime with pulse energy limited to 40 pJ at 60 MHz. The mode-locked spectrum exhibits Kelly-side bands typically associated with soliton pulses, shown in Fig. 1b; therefore, a pumped SSFS amplifier was used to smoothen and broaden the spectrum for further amplification.

## 2.2 Soliton self frequency shift amplifier

Output from the mode-locked oscillator propagated through a free space isolator and half-wave plate before being coupled into the single-mode PM 10/130 fiber input port of a 2 + 1:1 taper fiber bundle (TFB) (ITF Labs/3S Photonics), as shown in Fig. 2. The TFB was pumped with a 35 W, 793 nm diode (DILAS Diodenlaser GmbH) with 100  $\mu$ m diameter delivery fiber, and spliced to a  $\sim 5$  m long section of PM 10/130 Tm-doped fiber (Nufern). The active fiber was wrapped around a 11-cm water-cooled mandrel. This amplifier utilized a Raman-soliton self-frequency shift, where the output signal was tunable from 1,980 to 2,100 nm depending on the diode pump power. The output of this system produced an amplified pulse with a smooth spectrum, red-shifted from the oscillator center wavelength of 1,975 nm. The total output power was split between the residual oscillator pulse and the frequency shifted pulse, with  $\sim 60$  % of power in the shifted pulse. Figure 2 shows both the spectral and temporal characteristics corresponding to 3 nJ energy in the shifted soliton. During amplification, the pulse spectral width broadened to 30 nm (FWHM) and the autocorrelation confirms the

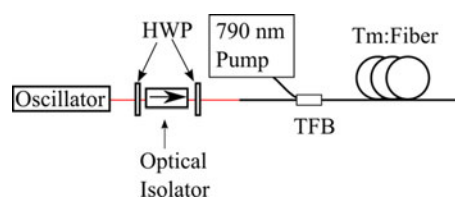


**Fig. 2** Schematic of the free space polarization components prior to the Raman amplifier

pulses are transform-limited with 150 fs (FWHM) pulse duration. The inset of Fig. 3 b) shows the autocorrelation on a longer time scale, where the signal from the residual oscillator pulse is evident  $\sim 2$  ps from the Raman-SSFS pulse.

## 2.3 Single mode amplifier

In order to amplify to higher energy, the pulses were temporally stretched in a CBG. The CBG reflectivity has a square 52 nm wide bandwidth (Fig. 4) centered at 2,020.5 nm, with both surfaces anti-reflection coated for 1,900–2,200 nm. The reflectivity averages 82 % across the full reflection bandwidth, and we calculated the group velocity dispersion is 12.3 ps<sup>2</sup> [16]. At this time, we are not able to measure the stretched pulse directly, but we estimate it to be  $\sim 160$  ps with normal dispersion stretching.

The schematic for the CPA stage of this laser system is shown in Fig. 5. The Raman-soliton was free space coupled to the amplifier stage after the pulse was stretched using the CBG. Using a quarter-wave plate (QWP), upon reflection from the CBG the polarization orientation was rotated 90° so that the stretched signal was output through the side facet of a polarizing beam splitter (PBS). The residual signal from the oscillator pulse centered at 1,975 nm was not reflected by the CBG and was therefore not amplified.

In order to compress the pulse to the minimum duration, a section of normal dispersion fiber was inserted to compensate the anomalous dispersion of the fiber in the amplifier; without this dispersion compensating fiber (DCF), the minimum compressed pulse duration was 4 ps. Due to the small

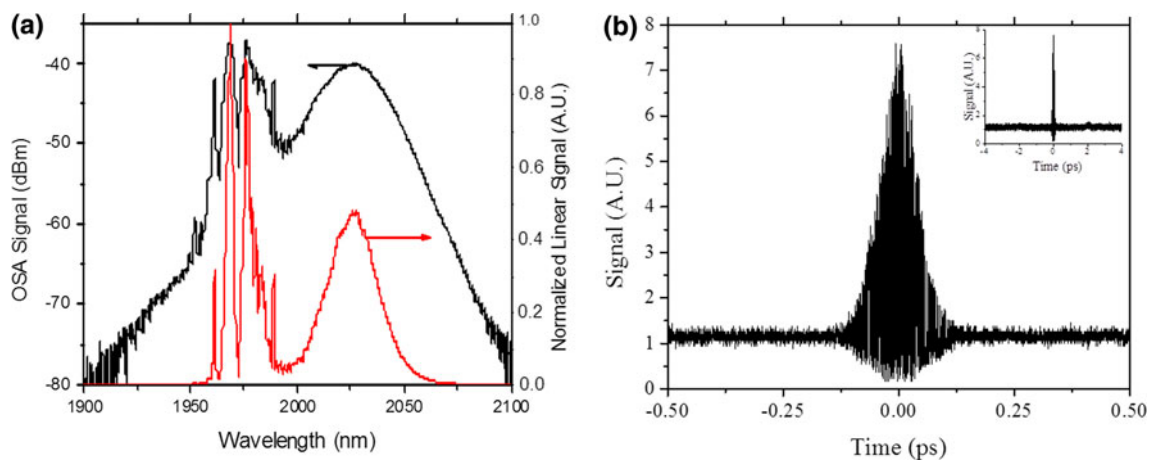


**Fig. 3** **a** This figure shows the output spectrum in linear and logarithmic scale as measured with an optical spectrum analyzer. **b** The interferometric autocorrelation shows the  $\sim 150$  fs duration of

the pulse. The *inset* extends the time scale, showing evidence of the input oscillator pulse  $\sim 2$  ps from the shifted pulse

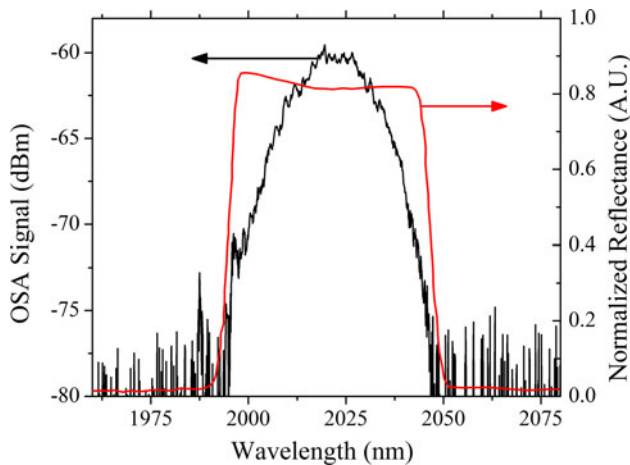


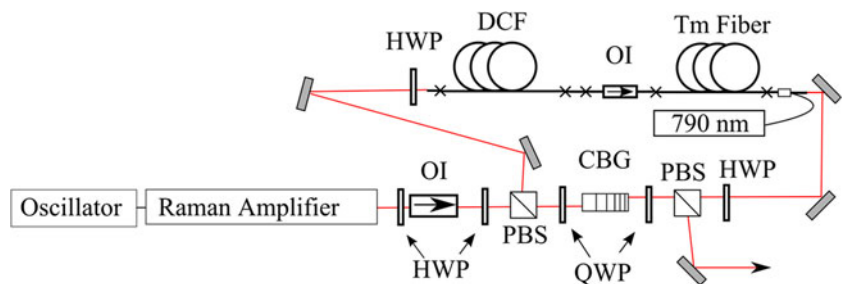
**Fig. 4** Pulse spectrum following the CBG. The *red curve* shows the reflectance of the CBG

mode-field diameter of the DCF, a mode field adaptor (MFA) was fabricated to couple the DCF to SM2000, a non-PM single-mode fiber with a 11/125  $\mu\text{m}$  core/cladding diameters, to maximize seed coupling into the amplifier. A  $\sim 9$  m section of DCF, bookended by MFAs, was inserted prior to the amplifier with  $\sim 1$  dB loss. The SM2000 fiber was spliced to the undoped fiber pigtail (PM 10/130) of a

polarization-dependent fiber-coupled optical isolator (Shinkosha Co.) to prevent any feedback from the amplifier and ensure linear polarization of light prior to amplification. The isolator was spliced to a 4 m section of Tm-doped PM 10/130 fiber that was wrapped around a water-cooled mandrel for thermal management during amplification. This single-mode amplifier was counter-propagation pumped using a 2 + 1:1 TFB. A final section of undoped PM 10/130 was spliced to the output single port of the TFB and cutback to fine balance the dispersion of the DCF and anomalous fiber in the cavity. The pulse was compressed in the CBG using the opposite facet from that for pulse stretching via polarization-dependent transmission (input) and reflection (output) from a PBS.

After stretching in the CBG, the power was  $\sim 120$  mW. Due to coupling losses from the CBG into the DCF as well as the insertion loss of the DCF and fiber isolator, we estimate the average power injected into the Tm: fiber amplifier was  $\sim 50$  mW. This was amplified to a maximum average power of 5.8 W with 10 % power in ASE, and was re-compressed to as short as 400 fs pulse duration. As shown in Fig. 6, there was a slight increase in pulse duration from 400 to 550 fs during amplification to 85 nJ, which we attribute to further truncation of the optical spectrum during compression.

**Fig. 5** Schematic of the stretching/compressing and single-mode amplifier. *OI* optical isolator, *HWP* half-wave plate, *QWP* quarter-wave plate, *PBS* polarizing beam splitter, *CBG* chirped volume Bragg grating, *DCF* dispersion compensating fiber



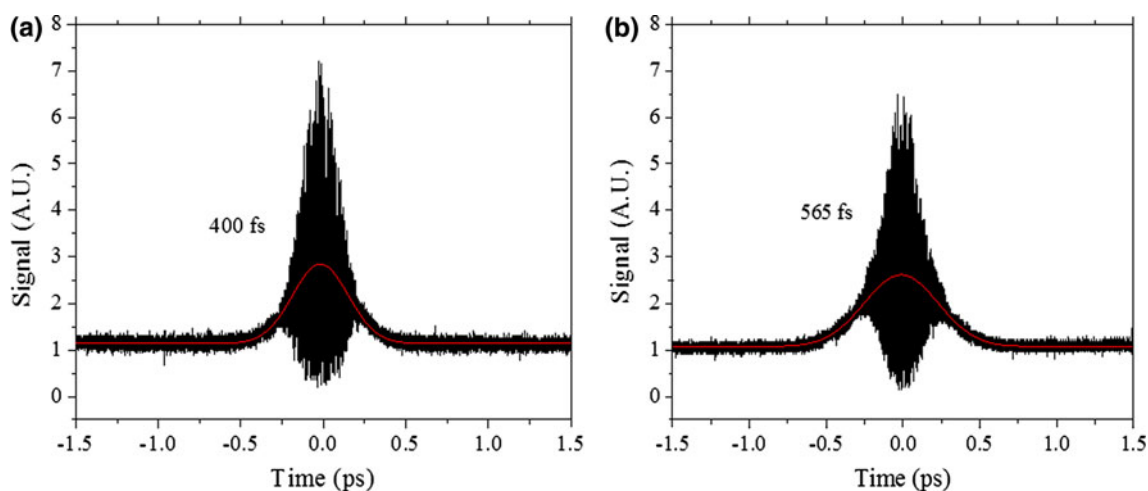


**Fig. 6** Interferometric autocorrelation of pulses show pulse duration of 400 and 565 fs at **a** low (30 nJ) and **b** high energy (85 nJ), respectively

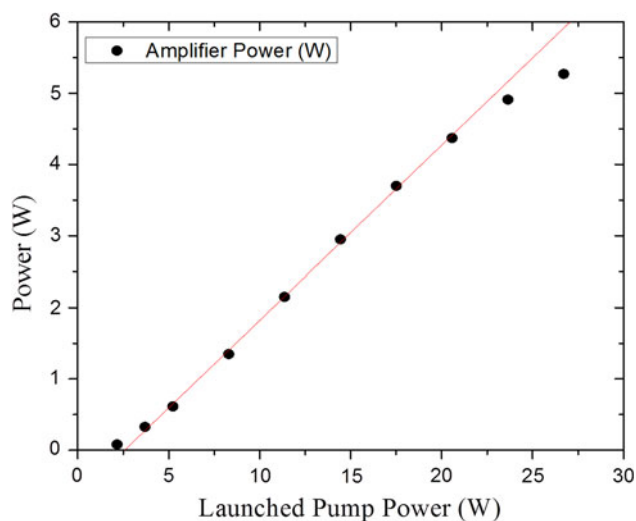


**Fig. 7** Amplifier output power with respect to launched pump power, corresponding to  $\sim 24\%$  slope efficiency

As shown in Fig. 7, there was a slight roll-off in the slope efficiency suggesting that  $\sim 20$  dB is the maximum gain possible for this single-stage single-mode fiber amplifier. As shown in Fig. 8a, there is no evidence of spectral modulation due to self-phase modulation or gain narrowing during amplification, and there is only a slight blue-shift of the center wavelength towards the ASE peak near 1,950 nm. Figure 8b shows the final spectrum after compression at 85 nJ. The output appears narrower than the corresponding case in Fig. 7a, because the beam is slightly spatially chirped by the CBG; therefore, the collection fiber for the OSA does not capture the full spectrum.

### 3 Discussion

One of the major limitations of fiber CPA systems is the maximum amount of nonlinear phase that can be

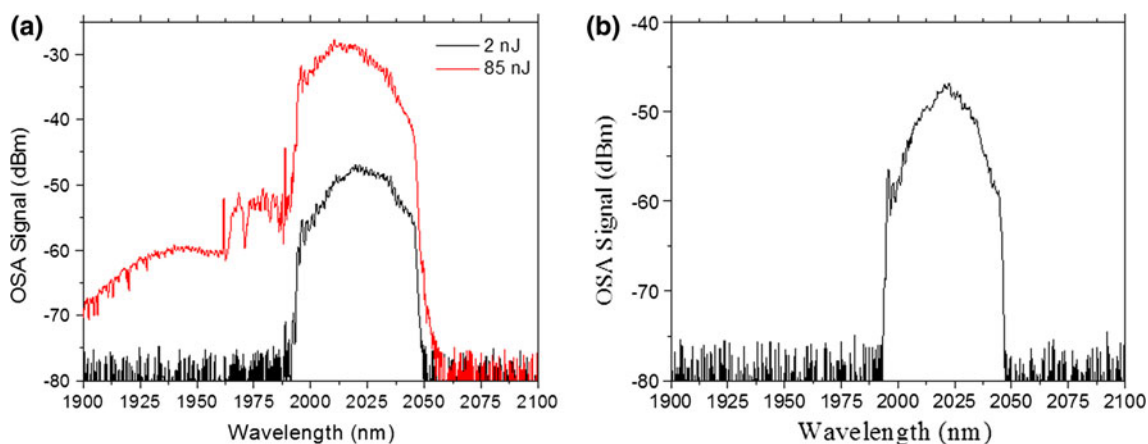


**Fig. 8** **a** The spectral output of the single-mode amplifier at both low and high energy prior to compression with the CBG. **b** The spectral output of the compressed pulses

accumulated before proper pulse compression is impossible, as quantified by the B-integral. We have modeled the pulse evolution in the single-stage amplifier using FiberDesk and calculated the B-integral to be  $\sim 1.3$  radians. Assuming a B-Integral limit of  $\pi$  radians, it should be possible to reach  $\sim 0.9 \mu\text{J}$  in this single-mode amplifier with this stretch pulse duration with negligible nonlinear spectral or temporal degradation.

Although the CBG is a simple and compact device providing temporal reciprocity for stretching and recompressing, it limits the maximum stretch pulse duration and the spectral bandwidth for CPA. In addition, the bandwidth of the Raman soliton and the reflectivity bandwidth of the CBG limit the minimum compressible pulse duration. The CBG has a rectangular shaped spectrum spanning 52 nm and the Raman soliton has a FWHM of 30 nm with a corresponding full width bandwidth  $>52$  nm. Thus, portions of the spectral wings of the input seed are truncated and the amplified pulse cannot be recompressed to the input pulse duration. Furthermore, the DCF compensates the GVD of the amplifier fiber; however, residual TOD and higher order dispersion are not cancelled. Figure 9 shows a computer simulation of the Fourier transform of a truncated hyperbolic secant and the initial hyperbolic secant pulse. The transform limited pulse duration (FWHM) increases from 150 to 272 fs between the hyperbolic secant and the truncated spectrum. Assuming the ideal case of a hyperbolic secant pulse shape, the time-bandwidth product of low energy pulses and 400 fs pulse duration are 0.704 and 0.98 at the highest energy. Taking into account the truncated spectrum, at high energy the pulse duration is double the time-bandwidth limit.

In order to verify and utilize the high peak power (150 kW) of the compressed pulses, we investigated

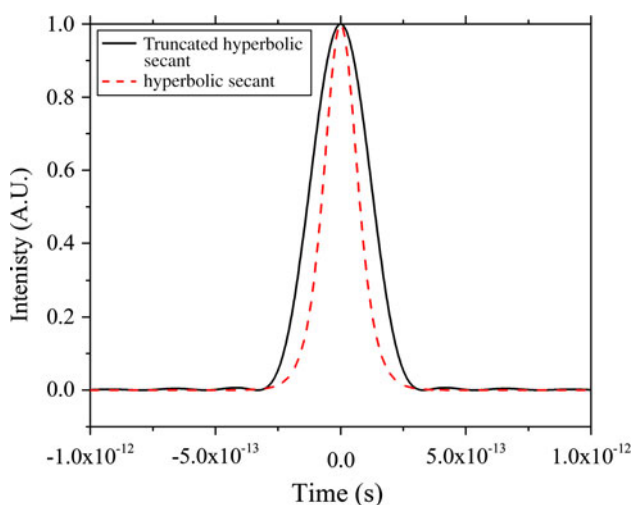


**Fig. 9** Fourier transform of a hyperbolic secant function and a truncated hyperbolic secant. This graph simulates the transform limited pulses expected with compression using a CBG

spectral broadening in a short section of highly nonlinear fiber. The fiber was made using tellurite glass with molar composition 73 %  $\text{TeO}_2$ –20 %  $\text{ZnO}$ –5 %  $\text{Na}_2\text{O}$ –2 %  $\text{La}_2\text{O}_3$  with a refractive index of 1.98 at  $1.5 \mu\text{m}$ . A more detailed description of the properties of the glass is given in [17]. To fabricate the fiber, we produced a suspended core preform and a jacket tube using the billet extrusion technique [18]. The glass billet for extrusion of the suspended core preform was melted in controlled dry atmosphere, which reduced the OH content by an order of magnitude compared with glass melted in open air [19]. The suspended core preform was first drawn down to a cane of  $\sim 2$  mm diameter, then the cane was inserted into the jacket tube having 10-mm outer diameter. Finally, the cane-in-tube assembly was drawn down to fiber, whereby the top of the cane was sealed to avoid hole closure via self-pressurization of the cane holes [20]. An SEM image of the fiber is shown in Fig. 10. The fiber has an outer diameter of  $200 \mu\text{m}$  and a core diameter of  $3.1 \mu\text{m}$ .

Compressed pulses were coupled into the tellurite fiber with  $\sim 10$  % coupling efficiency at input energies of 2 and 14 nJ corresponding to  $\sim 0.2$  and  $\sim 1.4$  nJ in the fiber, respectively. Figure 11 shows the output spectra for these two energies. Despite the  $\sim 90$  % coupling loss, at the maximum peak power in the fiber of  $\sim 3.5$  kW spectral broadening spanned 1,850–2,300 nm at the  $-20$  dB level. Simulation has shown that pumping similar  $\text{TeO}_2$  fibers with 75 kW peak power near the zero dispersion wavelength at  $1.93 \mu\text{m}$  should generate a broad supercontinuum from  $<1$  to  $>4 \mu\text{m}$  [2]. These results represent initial results with this non-optimized tellurite fiber, but we anticipate significant improvement through optimization of the zero dispersion wavelength and improvement of the pump coupling.

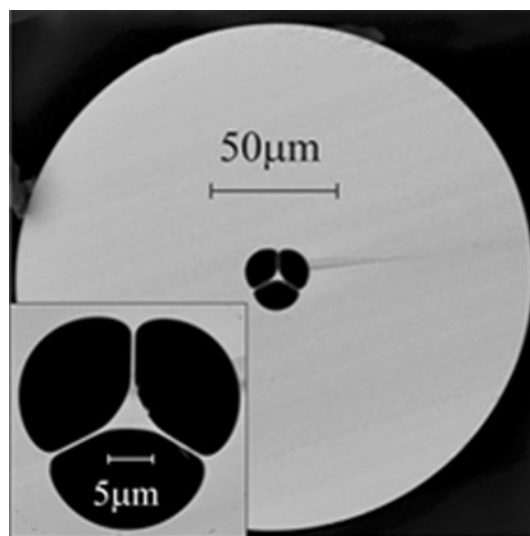


**Fig. 10** SEM image of the tellurite fiber used for spectral broadening

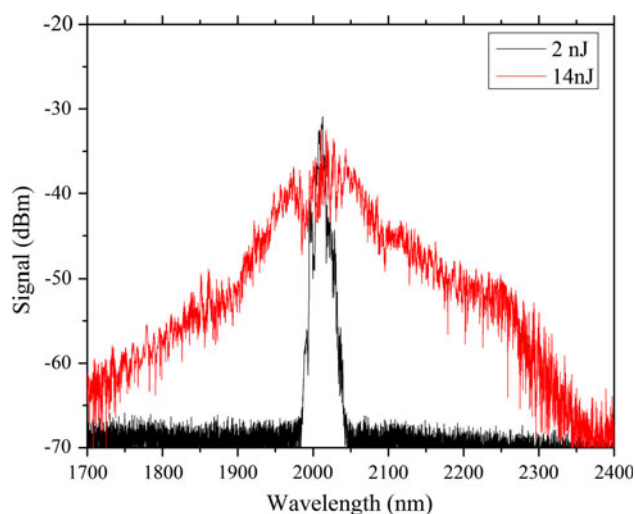


**Fig. 11** Spectral broadening in tellurite suspended core fiber

#### 4 Conclusion

In this work, we have demonstrated the generation and amplification of femtosecond pulses in thulium-doped fiber. To our knowledge, this is the first time that a CBG has been used to stretch and recompress pulses at wavelengths near 2  $\mu\text{m}$  and, it is clear that we have not yet reached the limits of CBG technology in terms of peak power or average power. The compressed pulses were input into a highly nonlinear fiber to demonstrate spectral broadening and confirm the utility of this ultrashort pulse Tm: fiber source for supercontinuum generation. The system will be the front end for ongoing efforts to further amplify in large mode-area to  $\mu\text{J}$ -energies and MW peak powers.

**Acknowledgments** The authors acknowledge the support of the Department of Defense (DoD) High Energy Laser Joint Technology Office (JTO) through the Multidisciplinary Research Initiative (MRI) program (contract #W911NF-05-1-0517), the Office of Naval

Research (ONR) through a Defense University Research Program (contract #N000141210144), and the State of Florida.

#### References

1. N. Leindecker, A. Marandi, R.L. Byer, K.L. Vodopyanov, I. Hartl, M. Fermann, P.G. Schunemann, *Opt. Exp.* **20**, 7046–7053 (2012)
2. D. Buccoliero, H. Steffensen, O. Bang, H. Ebendorff-Heidepriem, T.M. Monro, *Appl. Phys. Lett.* **97**, 061106 (2010)
3. L.E. Nelson, E.P. Ippen, H.A. Haus, Broadly tunable sub-500 fs pulses from an additive-pulse mode-locked thulium-doped fiber ring laser. *Appl. Phys. Lett.* **67**, 19 (1995)
4. R.C. Sharp, D.E. Spock, N. Pan, J. Elliot, *Opt. Lett.* **21**, 881–883 (1996)
5. M.A. Solodyankin, E.D. Obraztsova, A.S. Lobach, A.I. Chernov, A.V. Tausenev, V.I. Konov, E.M. Dianov, *Opt. Lett.* **33**, 1336–1338 (2008)
6. M. Engelbrecht, F. Haxsen, A. Ruehl, *Opt. Lett.* **33**, 690–692 (2008)
7. R. Sims, P. Kadwani, L. Shah, M. Richardson, *ASSP* **4**, ATuD4 (2011)
8. S. Kivisto, T. Hakulinen, *IEEE Phot. Tech. Lett.* **19**, 934–936 (2007)
9. G. Imeshev, M. Fermann, *Opt. Exp.* **13**, 7424–7431 (2005)
10. F. Haxsen, D. Wandt, U. Morgner, J. Neumann, D. Kracht, *Opt. Lett.* **35**, 2991–2993 (2010)
11. L.-M. Yang, P. Wan, V. Protopopov, J. Liu, *Opt. Exp.* **20**, 5683–5688 (2012)
12. C.R. Phillips, J. Jiang, C. Mohr, A.C. Lin, C. Langrock, M. Snure, D. Bliss, M. Zhu, I. Hartl, J.S. Harris, M.E. Fermann, M.M. Fejer, *Opt. Lett.* **37**, 2928–2930 (2012)
13. K.-H. Liao, M.-Y. Cheng, E. Flecher, V.I. Smirnov, L.B. Glebov, A. Galvanauskas, *Opt. Exp.* **15**, 4876–4882 (2007)
14. G. Chang, M. Rever, V. Smirnov, *Opt. Lett.* **34**, 2952–2954 (2009)
15. K. Kieu, M. Mansuripur, *Opt. Lett.* **32**, 2242–2244 (2007)
16. F. Ouellette, *Opt. Lett.* **12**, 847–849 (1987)
17. M.R. Oermann, H. Ebendorff-Heidepriem, Y. Li, T.-C. Foo, T.M. Monro, *Opt. Exp.* **17**, 15578–15584 (2009)
18. H. Ebendorff-Heidepriem, T.M. Monro, *Opt. Mat. Exp.* **2**, 304 (2012)
19. H. Ebendorff-Heidepriem, K. Kuan, M.R. Oermann, K. Knight, T.M. Monro, *Opt. Mat. Exp.* **2**, 432 (2012)
20. C.J. Voyce, A.D. Fitt, J.R. Hayes, T.M. Monro, *J. Light. Tech.* **27**, 871–878 (2009)